Time resolved confocal luminescence investigations on Reverse Proton Exchange Nd:$LiNbO_3$ channel waveguides

E. Martín Rodríguez,[1] D. Jaque,[1*] E. Cantelar,[1] F. Cussó,[1] G. Lifante,[1] A.C. Busacca,[2] A.C. Cino,[2,3] and S. Riva Sanseverino [2,3]

[1] *Departamento de Física de Materiales, Facultad de Ciencias, Universidad Autónoma de Madrid, 28049-Madrid, Spain*

[2] *DIEET, Università degli Studi di Palermo, v.le delle Scienze Ed. 9, 90128-Palermo, Italy*

[3] *Centro per la Ricerca Elettronica in Sicilia (CRES), Via Regione Siciliana 49, 90046-Monreale (PA), Italy*

[*] *Corresponding author: daniel.jaque@uam.es*

Abstract: In this work we report on the time and spatial resolved fluorescence of Neodymium ions in $LiNbO_3$ channel waveguides fabricated by Reverse Proton Exchange. The analysis of the fluorescence decay curves obtained with a sub-micrometric resolution has evidenced the presence of a relevant fluorescence quenching inside the channel waveguide. From the comparison between diffusion simulations and the spatial dependence of the $^4F_{3/2}$ fluorescence decay rate we have concluded that the observed fluorescence quenching can be unequivocally related to the presence of H^+ ions in the $LiNbO_3$ lattice. Nevertheless, it turns out that Reverse Proton Exchange guarantees a fluorescence quenching level significantly lower than in similar configurations based on Proton Exchange waveguides. This fluorescence quenching has been found to be accompanied by a relevant red-shift of the $^4F_{3/2} \rightarrow {}^4I_{9/2}$ fluorescence band.

OCIS codes: (130.3730) Lithium Niobate; (160.3380) Laser materials; (230.7370) Waveguides.

References and links

1. L. Arizmendi, "Photonic applications of Lithium Niobate" Phys. Stat. Solidi A **201**, 253-283 (2004)
2. P. Baldi, M. De Micheli, K. El Hadi, A. C. Cino, P. Aschieri, and D. B. Ostrowsky, "Proton exchanged waveguides in $LiNbO_3$ and $LiTaO_3$ for integrated lasers and nonlinear frequency converters," Opt. Eng. **37**, 1193-1202 (1998).
3. J. L. Jackel, C. E. Rice, and J. J. Veselka, "Proton exchange for high-index waveguides in $LiNbO_3$" Appl. Phys. Lett. **41**, 607-608 (1982).
4. E. Lallier, J. P. Pocholle, M. Papuchon, C. Grezes-Besset, E. Pelletier, M. De Micheli, M. J. Li, Q. He and D. B. Ostrowsky, "Laser oscillation of single-mode channel waveguide in Nd: MgO:$LiNbO_3$"Electron. Lett. **25**, 1491-1492 (1989).
5. J. L. Jackel, C. E. Rice, and J. J. Veselka, "Proton exchange for highindex waveguides in $LiNbO_3$," Appl. Phys. Lett. **41**, 607-608 (1982).
6. E. Lallier. "Lasers guides dóndes dans le Niobate de Lithium dope Neodyme," Universite de Paris-Sud, PhD Thesis (1992).
7. J. L. Jackel, and J. J. Johnson, "Reverse exchange method for burying proton exchanged waveguides," "Electron. Lett. **27**, 1360-1361 (1991).
8. Y. N. Korkishko, V. A. Fedorov, T. M. Morozova, F. Caccavale, F. Gonella, and F. Segato, "Riverse proton exchange for buried waveguides in LiNbO3," J. Opt. Soc. Am. A **15**, 1838-1842 (1998).
9. A. Di Lallo, C. Conti, A. Cino, and G. Assanto, "Efficient Frequency Doubling in Reverse Proton Exchanged Lithium Niobate waveguides," IEEE Photon. Technol. Lett. **13**, 323-325, (2001).
10. J. Olivares and J.M. Cabrera. "Guided modes with ordinary refractive index in proton exchanged $LiNbO_3$ waveguides," Appl. Phys. Lett. **62**, 2468-2470 (1993).
11. K. R. Parameswaran, R. K. Route, J. R. Kurz, R. V. Roussev, M. M. Fejer and M. Fujimura. "Highly efficient second-harmonic generation in buried waveguides formed by annealed and reverse proton exchange in periodically poled lithium Niobate," Opt. Lett. **27**, 179-181 (2002).

#82717 - $15.00 USD Received 3 May 2007; revised 25 Jun 2007; accepted 26 Jun 2007; published 28 Jun 2007

12. M. Domenech, G. Lifante and F. Cussó, A. Parisi, A.C. Cino and S. Riva Sanseverino, "Fabrication and characterisation of reverse proton exchange optical waveguides in Neodymium doped lithium niobate crystals," Materials Science Forum. **480-481**, 429-436 (2005)
13. G. Lifante, E. Cantelar, F. Cussó, M. Domenech, A.C. Busacca, A.C. Cino and S. Riva Sanseverino "Imaginary distance BPM as an efficient tool for modelling optical waveguides fabrication by ion diffusion," Proc. OWTNM'06, Varese, Italy (2006)
14. C. Jacinto, S. L. Oliveira, L. A. O. Nunes, T. Catunda, and M. J. V. Bell. "Thermal lens study of the OH^- influence on the fluorescence efficiency of Yb^{3+}-doped phosphate glasses," Appl. Phys. Lett. **86**, 071911 (2005).
15. U. R. Rodríguez Mendoza, A. Ródenas, D. Jaque, I. R. Martín, F. Lahoz and V. Lavín "High pressure luminescence in Nd doped $LiNbO_3$ crystals," High Press. Res. Journal.**26**, 341-343 (2006)
16. D. Jaque, E. Cantelar and G. Lifante "Lattice micro-modifications induced by Zn difussion in Nd:LiNbO3 channel waveguides probed by Nd^{3+} confocal luminescence," Appl. Phys. B. DOI: 10.1007/s00340-007-2692-9 (2007).
17. B. V. Dierold and C. Sandmann. "Inspection of periodically poled waveguide devices by confocal luminescence microscopy," Appl. Phys. B. **78**, 363-366 (2004).

1. Introduction

$LiNbO_3$ is a well-known and widely used crystal because of its good electro-optical, acoustico-optical and nonlinear properties. The combination of such properties with the laser gain of Nd^{3+} ions in the same medium has permitted the construction of many interesting systems including self Q-switched, self mode-locked and self frequency converters laser devices [1]. For those applications involving non linear optical conversion processes the channel waveguide design is of special relevance since the achievement of high spatial overlap and confinement of both pump and second order waves leads to a strong enhancement in the optical conversion efficiencies. For the same reason, the guided configuration is also advantageous for lasing devices, when low threshold and compact size are required [2]. Among the different methods available for Nd:$LiNbO_3$ channel waveguide fabrication, Proton Exchanged (PE) waveguides have focused much attention because of the low loss, high index contrast and photorefractive resistant waveguides that can be obtained [3]. As a matter of fact the first single mode channel waveguide laser was demonstrated using this technique on a Nd:MgO:$LiNbO_3$ substrate [4]. Despite of the good results obtained in PE Nd^{3+} doped $LiNbO_3$ channel waveguides, they present two drawbacks: i) first they only support extraordinary mode propagation [5], thus seriously limiting its application in frequency converter devices for which both TE and TM radiations are involved; ii) secondly, previous works have stated that PE procedure causes a remarkable reduction in the $^4F_{3/2}$ lifetime. As a matter of fact lifetime reductions as large as 60 % (from 90 μs down to 30 μs) have been reported [6]. This lifetime reduction is an undesirable feature for laser applications as it leads to a noticeable increment in the laser threshold. Furthermore, this lifetime reduction is expected to follow a strong spatial dependence, this producing a non homogeneous laser gain within the channel waveguide.

Reverse Proton Exchange (RPE) has emerged as an alternative method for the fabrication of channel waveguides in Nd^{3+} doped $LiNbO_3$ waveguides. RPE procedure has been reported to lead to low losses buried and symmetric $LiNbO_3$ channel waveguides able to confine the two principal (orthogonal) polarizations [7-10]. These facts make RPE $LiNbO_3$ channel waveguides of major interest in the realization of rare earth doped lasing configurations as well as highly efficient one and two dimensional nonlinear devices due to the good matching of the interacting modes field profiles within the waveguide [11]. Despite of its interest and potential applications, the actual influence of the RPE process on the spectroscopic properties (especially on the $^4F_{3/2}$ fluorescence lifetime) of Neodymium ions is still an almost unexplored question [12]. In this work we have applied the Time Resolved Confocal Luminescence (TRCL) technique to the study of the luminescence properties of Nd^{3+} ions in RPE channel waveguides fabricated in $LiNbO_3$ crystals. The information extracted in this way is of great relevance from the application point of view (laser performance is determined by the

#82717 - $15.00 USD Received 3 May 2007; revised 25 Jun 2007; accepted 26 Jun 2007; published 28 Jun 2007

spectroscopic properties of Nd^{3+} ions) and also from a fundamental point of view if a relation between spectroscopic changes and the proton distribution can be established.

2. Experimental

Z-cut $LiNbO_3$ wafers bulk doped with 0.2 mol% of Nd^{3+} ions ($3.78x10^{19}$ ions/cm^3) and dimensions of 8.5x10x1 mm^3 have been cut and polished up to optical quality. Channels of 17 μm width were defined on a silica mask by using standard photolithographic techniques. Figure 1(a) shows a schematic drawing of the cross section view of the channel mask opening, where the exchange can take place during waveguide fabrication. The reference system used all along this work is also indicated. We have defined the "*x*" axis as parallel to the diffusion surface, being the origin ($x = 0$) located at the air-waveguide interface. The "*y*" axis is then perpendicular to this interface. In this case $y = 0$ is set to be at the centre of the studied SiO_2 channel, whose width is denoted by *w*. The optical waveguides have been fabricated following the RPE technique. For that purpose, a first PE stage was performed in benzoic acid at 300ºC during 14.5 hours with the sealed ampoule technique. In order to produce optical waveguides that support both quasi-$TM_{0,0}$ and quasi-$TE_{0,0}$ propagating modes around 1 μm wavelength, a second step (RPE stage) was performed. In this stage, the sample was immersed in a mixture of Li/Na/K nitrides at 350ºC during 38.5 hours [7-8]. In this case, the usual m-lines spectroscopic characterization only can give direct information relative to the ordinary waveguide (TE propagating modes) close to the surface, for example through IWKB calculation. The buried extraordinary waveguide can be modeled with different numerical approach, such as the imaginary distance BPM [13]. Figure 1(b) shows the 2D proton density as obtained by solving the diffusion equations that governs the diffusion processes of the two involved species (H^+ and Li^+), by this finite difference approach. The calculation of Fig. 1(b) reveals that the initially sharp proton profile characteristic of PE waveguides is smoothed by the RPE technique. Close to the surface, proton out-diffusion mechanisms reduce the proton concentration recovering partially the initial refractive indices of the wafer. On the other hand, the higher temperature used in the RPE gives rise to a redistribution of protons further into the substrate: as consequence a region doped with a moderate proton concentration remains buried in the wafer below the mask opening. The refractive indices of this buried region are such that the extraordinary and ordinary refractive indices are higher and lower, respectively, than those of the initial wafer. Therefore, this region allows the optical confinement of TM propagating modes while it represents an optical barrier of low refractive index for the TE propagating modes, which are confined between the sample surface and this optical barrier.

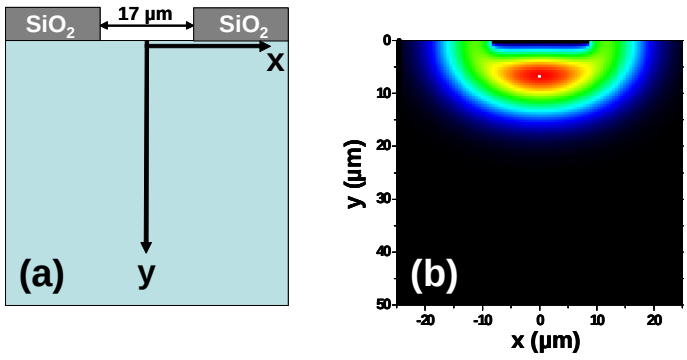

Fig. 1. (a).- Nd:LiNbO3 sample with silica mask channel opening. Reference axis used in this work are indicated. (b).- Two dimensional calculation of the proton density in the waveguide as obtained by using the imaginary distance beam propagation method

#82717 - $15.00 USD Received 3 May 2007; revised 25 Jun 2007; accepted 26 Jun 2007; published 28 Jun 2007

For TRCL experiments we have used an Olympus BX41 fiber coupled microscope. The exciting source was, for all the experiments, a 0.2-mm fibre coupled 808 nm laser diode (LIMO GmbH). The diode was operating in pulsed mode providing 50 μs pulses with a repetition rate of 2.5 kHz. For this excitation wavelength the Nd^{3+} ions were excited through the $^4I_{9/2} \rightarrow {}^4F_{3/2}$ transition, giving rise to the subsequent $^4F_{3/2} \rightarrow {}^4I_{9/2}$, $^4I_{11/2}$ and $^4I_{13/2}$ fluorescence transitions. The 808 nm excitation beam was focused by using a 100X microscope objective. The Nd^{3+} fluorescence was collected by the same focusing objective and focused into a 50 μm diameter fibre. A variable pinhole was positioned between the microscope objective and the collection fibre to ensure a confocal operation scheme. For lifetime measurements the collection fibre was connected to a photomultiplier tube and the generated signal was averaged and recorded by a 500 MHz Lecroy digital oscilloscope. For the spectral analysis of the Nd^{3+} luminescence the collection fibre was connected to a CVI spectrometer. The waveguide was mounted onto an XY motorized stage with 0.1 μm spatial resolution. All the experiments were carried out at room temperature. The spatial resolution in the confocal configuration here described and the uncertainty in the lifetime determination was estimated to be 0.7 μm and ± 2%, respectively.

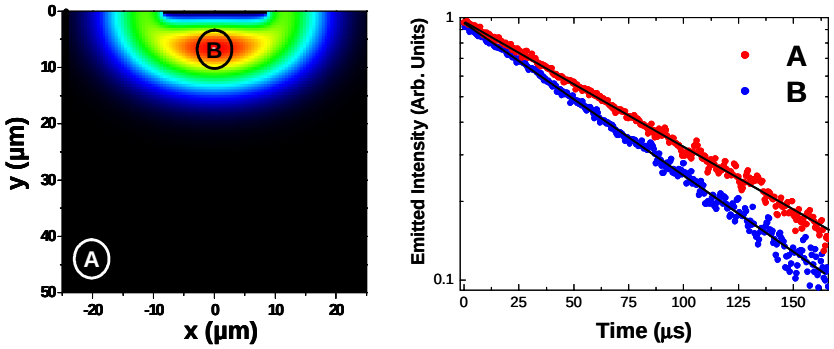

Fig. 2.- Fluorescence decay curve of the $^4F_{3/2}$ metastable state of Nd^{3+} ions in the $LiNbO_3$ bulk and RPE channel waveguide (red and blue points, respectively). Solid lines correspond to a single exponential fit. The spatial location at which each curve was measured is indicated in the graph on the left.

3. Results and discussion

Figure 2 shows the $^4F_{3/2}$ fluorescence decay curves obtained close (exchange region) and far away (no exchange region) from the SiO_2 channel opening used to define the RPE channel waveguide. From this Figure a clear reduction in the $^4F_{3/2}$ fluorescence lifetime (from 90 down to 78 μs) can be observed. In order to get a further understanding on the origin of this lifetime reduction we have measured the $^4F_{3/2}$ fluorescence lifetime along both the (x, y =3 μm) and (x=0, y) directions (Figures 3(a) and 3(a), respectively). The calculated density of protons along these two directions has been also included as green solid lines in Fig. 3(a) and 3(b). From these Figures a clear connection between the reduction in the Nd^{3+} fluorescence lifetime and the presence of protons is deduced [11]. In Fig. 3(a) the maximum reduction in the $^4F_{3/2}$ fluorescence lifetime is achieved 6 μm below the sample surface, this being the in depth distance at which the density of protons achieve its maximum value. Furthermore, the reduction in the $^4F_{3/2}$ fluorescence lifetime extends over 20 μm, in good agreement with the penetration depth calculated for protons. The strong relation between proton presence and the Neodymium fluorescence lifetime reduction is also evidenced from the comparison between experimental data and calculations obtained along the (x = 0, y) scan direction (Fig. 3(b)). In this case the maximum fluorescence lifetime reduction is achieved for x = 0, where the proton

#82717 - $15.00 USD Received 3 May 2007; revised 25 Jun 2007; accepted 26 Jun 2007; published 28 Jun 2007

density is maximum. Furthermore, the "lateral" proton diffusion length (17 μm) also matches with the spatial extension of the Nd^{3+} fluorescence quenching.

The strong link between proton density and Neodymium fluorescence quenching (i.e. the reduction in the $^4F_{3/2}$ fluorescence lifetime) clearly stated by Fig. 3, can be explained by taking into account that the incorporated protons induce high energy vibration modes. As a consequence the multiphonon decay rate could be increased, leading to a reduction in the $^4F_{3/2}$ fluorescence lifetime. In addition it is known that the presence of OH^- groups in rare earth doped crystals and glasses could behave as energy acceptors in such a way that energy transfer processes are activated, thus leading to an additional increase in the non radiative decay rates [14]. One of these two mechanisms (or a combination of them) makes the luminescence to decay faster in the RPE waveguide, with a stronger lifetime reduction in the extraordinary waveguide, which corresponds to the highest proton concentration layer, while in the ordinary waveguide (TE modes) confined in the layer partially recovered during the Li→H second stage, the lifetime reduction is attenuated. The maximum lifetime reduction (from 90 down to 78 μs) represents a net decrease of about 14%, being this remarkable lower than that previously reported for PE waveguides (as high as 60 %) [6]. We state that this improvement is related with the reduction of "interstitial" protons introduced in the crystal after RPE procedure due to the second stage in which Li→H exchange takes place in combination with a relevant annealing.

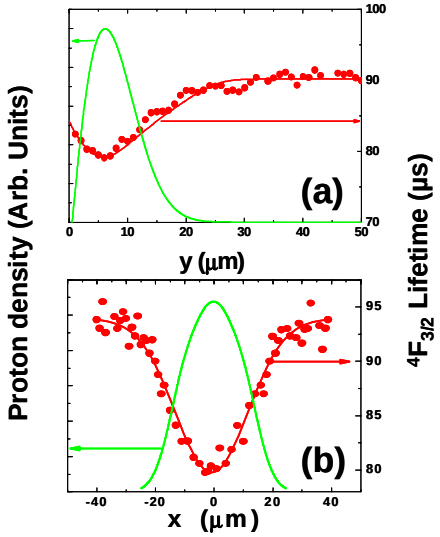

Fig. 3.- $^4F_{3/2}$ lifetime as a function of both *y* and *x* positions ((a) and (b), respectively). Green line corresponds to the proton density along the *y* and *x* scan directions.

In order to get a further understanding on the effects that RPE process has on the spectroscopic properties of Nd^{3+} ions we have also analyzed in detail the continuous wave $^4F_{3/2}\rightarrow{}^4I_{9/2}$ luminescence spectra. For this purpose the collection fiber was connected to a CVI-240 spectrometer and the 808 nm laser diode was operated in continuous wave mode. A band-pass filter was placed between the microscope objective and the collection fiber in order to block the strong 808 nm pumping scattering. Figure 4(a) shows a typical luminescence spectrum obtained. Note that some of the sub-stark transitions corresponding to the $^4F_{3/2}\rightarrow{}^4I_{9/2}$ luminescence channel are not present due to the spectral response of the filter used. Figure 4(b) shows the $^4F_{3/2}\rightarrow{}^4I_{9/2}$ integrated luminescence obtained along the "y" scan direction, revealing a decrease in the fluorescence efficiency of Nd^{3+} ions for distances below 20 μm and showing a minimum fluorescence emission at around 6μm where the density of protons reaches its maximum. Data shown in Fig. 4(b) are in good agreement with those included in

#82717 - $15.00 USD Received 3 May 2007; revised 25 Jun 2007; accepted 26 Jun 2007; published 28 Jun 2007

Fig. 3(a); the reduction in the fluorescence $^4F_{3/2}$ induced by the proton incorporation leads to a decrease in the storage ability of the metastable state. Therefore, under continuous wave excitation, the steady population of the metastable state is reduced, thus leading to a decrease in the fluorescence intensity.

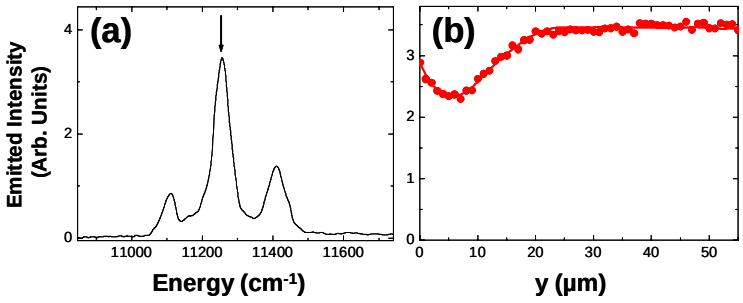

Fig. 4. (a).- $^4F_{3/2}\rightarrow{}^4I_{9/2}$ micro fluorescence spectrum obtained under continuous wave excitation. (b).- $^4F_{3/2}\rightarrow{}^4I_{9/2}$ emitted intensity as a function of the *y* position.

Additionally, we have also analyzed the energy position of the most intense luminescence peak within the $^4F_{3/2}\rightarrow{}^4I_{9/2}$ emission band (indicated by an arrow in Fig. 4(a)). Results have been displayed in Figure 5. For the sake of comparison we have also included the proton density along the y scan direction as obtained from Fig. 1 (b). Data included in Fig. 5 clearly indicate that the incorporation of protons during the waveguide fabrication process has induced changes in the spectral position of the Nd^{3+} luminescence bands. In particular we have obtained that for distances between 0 and 25 μm a blue shift has been induced, being the maximum of this blue shift located at around 6 μm. From Fig. 5 it is clear that the blue shift of Nd^{3+} luminescence (red symbols) follows the proton density (green line). According to previous works, this blue shift reflects a local dilatation of the $LiNbO_3$ lattice [15,16]. Thus, we can conclude from Fig. 5 that the incorporation of protons in RPE $LiNbO_3$ waveguides leads to local lattice dilatation. Finally it should be mentioned that the maximum Nd^{3+} blue shift obtained in RPE $LiNbO_3$ waveguides ($\approx$ 0.8 cm^{-1}) is lower that that recently reported for Zn diffused Nd:$LiNbO_3$ waveguides ($\approx$ 2 cm^{-1}) [16], thus indicating a reduced lattice dilatation in the case of RPE $LiNbO_3$ channel waveguides. At this point it is important to note that energy shift of rare earth ions have been reported also in $LiNbO_3$ channel waveguides fabricated by other methods such as Ti indiffusion [17].

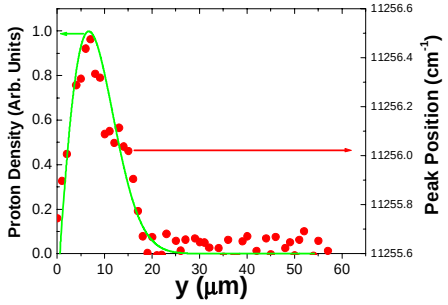

Fig. 5.- Energy position of the main luminescence peak within the $^4F_{3/2}\rightarrow{}^4I_{9/2}$ fluorescence band as a function of the *y* position (red points). Green line is the proton density as obtained from the 2D calculations included in Fig. 1(b).

#82717 - $15.00 USD Received 3 May 2007; revised 25 Jun 2007; accepted 26 Jun 2007; published 28 Jun 2007

4. Conclusions

In summary, the Time Resolved Confocal Luminescence has been applied to the study the spectroscopic properties of Neodymium ions in Reverse Proton Exchange channel waveguides. We have found that the proton incorporation leads to a remarkable modification in the $^4F_{3/2}$ metastable state life time. The analysis of the spatial dependence of the the $^4F_{3/2}$ metastable state life time has revealed a strong link between the lifetime reduction and the density of protons incorporated into the $LiNbO_3$ lattice. In the positions in which the maximum proton density has been achieved, the the $^4F_{3/2}$ metastable state life time is reduced down to 78 μs, this corresponding to a net decrease of ≈ 13 % (from 90 down to 78 μs). This reduction has been found to be less critical than that previously reported for Nd:$LiNbO_3$ Proton Exchange channel waveguides (as high as 60 %). This fact has been explained by taking into account the reduction in the density of "interstitial" protons that is produced by the Reverse Exchange process. Continuous wave experiments have revealed that the proton induced reduction in the $^4F_{3/2}$ metastable state lifetime also leads to a decrease in the fluorescence efficiency of Nd^{3+} ions which is also well correlated with the calculated spatial variation of proton density. Finally, we have also found that the waveguide formation procedure also leads to a blue shift of the Neodymium fluorescence bands. This effect has been tentatively related to a permanent lattice dilatation of the $LiNbO_3$ lattice. Results included in this work provide new information concerning the spectroscopic parameters of relevance in laser dynamics which could be of great interest for the future modeling and development of Nd:$LiNbO_3$ laser waveguides fabricated by Reverse Proton Exchange.

Acknowledgments

This work has been supported by the Spanish Ministerio de Ciencia y Tecnologia MAT2004-03347 and MAT2005-05950, by the UAM-Comunidad de Madrid (project CCG06-UAM/MAT-0347), by the Comunidad Autónoma de Madrid (CAM) under Projects S-0505-TIC-0191 and by the Italian MIUR with a PRIN 2005 project.

#82717 - $15.00 USD Received 3 May 2007; revised 25 Jun 2007; accepted 26 Jun 2007; published 28 Jun 2007